Translational Oncology

www.transonc.com

Volume 6 Number 6 December 2013 pp. 766–774 766

Impact of Perfusion Map Analysis on Early Survival Prediction Accuracy in Glioma Patients[1]

Benjamin Lemasson*, Thomas L. Chenevert*, Theodore S. Lawrence†, Christina Tsien†, Pia C. Sundgren*,‡, Charles R. Meyer*,§, Larry Junck¶, Jennifer Boes*, Stefanie Galbán†, Timothy D. Johnson#, Alnawaz Rehemtulla*,†, Brian D. Ross* and Craig J. Galbán*

*Department of Radiology, Center for Molecular Imaging, University of Michigan, Ann Arbor, MI; †Department of Radiation Oncology, Center for Molecular Imaging, University of Michigan, Ann Arbor, MI; ‡Department of Diagnostic Radiology, Clinical Sciences, Lund University, Lund, Sweden; §Department of Biomedical Engineering, Center for Molecular Imaging, University of Michigan, Ann Arbor, MI; ¶Department of Neurology, Center for Molecular Imaging, University of Michigan, Ann Arbor, MI; #Department of Biostatistics, Center for Molecular Imaging, University of Michigan, Ann Arbor, MI

Abstract

Studies investigating dynamic susceptibility contrast magnetic resonance imaging–determined relative cerebral blood volume (rCBV) maps as a metric of treatment response assessment have generated conflicting results. We evaluated the potential of various analytical techniques to predict survival of patients with glioma treated with chemoradiation. rCBV maps were acquired in patients with high-grade gliomas at 0, 1, and 3 weeks into chemoradiation therapy. Various analytical techniques were applied to the same cohort of serial rCBV data for early assessment of survival. Three different methodologies were investigated: 1) percentage change of whole tumor statistics (i.e., mean, median, and percentiles), 2) physiological segmentation (low rCBV, medium rCBV, or high rCBV), and 3) a voxel-based approach, parametric response mapping (PRM). All analyses were performed using the same tumor contours, which were determined using contrast-enhanced T1-weighted and fluid attenuated inversion recovery images. The predictive potential of each response metric was assessed at 1-year and overall survival. PRM was the only analytical approach found to generate a response metric significantly predictive of patient 1-year survival. Time of acquisition and contour volume were not found to alter the sensitivity of the PRM approach for predicting overall survival. We have demonstrated the importance of the analytical approach in early response assessment using serial rCBV maps. The PRM analysis shows promise as a unified early and robust imaging biomarker of treatment response in patients diagnosed with high-grade gliomas.

Translational Oncology (2013) 6, 766–774

Address all correspondence to: Craig J. Galbán, PhD, Assistant Professor of Radiology, Center for Molecular Imaging, University of Michigan, Biomedical Sciences Research Building, Room D200, 109 Zina Pitcher Place, Ann Arbor, MI 48109-2200. E-mail: cgalban@umich.edu

[1]This work was supported by the US National Institutes of Health research grants P01CA085878, U01CA166104, and P01CA087634. B.D.R. and A.R. have ownership interest (including patents) from Imbio, LLC. B.D.R., A.R., T.L.C., and C.J.G. have a financial interest in the underlying voxel-based technology. The other authors disclosed no potential conflicts of interest.

Received 21 October 2013; Revised 21 October 2013; Accepted 28 October 2013

 1944-7124/13

DOI 10.1593/tlo.13670

Introduction

Glioblastoma multiforme is the most common form of brain malignancy in adult patients, with approximately 53% of patients with primary brain tumors afflicted by this subtype [1]. Even with advancements in the clinical management of these patients, assessment of therapeutic response continues to be based on late or serial changes in tumor volume as measured by computed tomography or magnetic resonance imaging (MRI) [2,3]. The Macdonald criteria have been the standard for response assessment over the past 20 years [2], with changes in tumor volume of interest assessed on T1-weighted post-gadolinium (Gd-VOI) images acquired after the completion of chemoradiotherapy. It has become increasingly apparent that significant limitations exist in the Macdonald criteria, such as pseudoprogression that occurs in 20% to 30% of all newly diagnosed glioma patients treated with chemoradiation [4,5]. In 2010, the Response Assessment in Neuro-Oncology (RANO) Working Group sets new guidelines for response assessment in patients with glioma. In recognition that contrast enhancement is nonspecific and may not always serve as a surrogate of tumor response, these new assessment criteria incorporate non-enhancing imaging modalities such as fluid attenuated inversion recovery (FLAIR) images in addition to gadolinium-enhanced T1-weighted (T1-Gd) images to delineate brain tumors [3]. Although these new guidelines compensate for some of the deficiencies of the Macdonald criteria, RANO continues to rely on changes in tumor volume as determined on anatomic images that inevitably will introduce errors associated with interobserver variability [6]. To account for this, the guidelines also stipulate that it is permissible to acquire interval exams if radiographic changes are equivocal. For those patients nonresponsive to therapy, this would delay any change in their treatment management. With a median survival of only 14 months [7], such a delay could prove detrimental to the overall survival of the patient.

Functional imaging techniques show promise for diagnosis and assessment of treatment response of patients with cancer [8–11]. The relative cerebral blood volume (rCBV) as determined by dynamic susceptibility contrast (DSC) MRI has been shown to correlate with treatment efficacy in patients with glioma, providing a possible alternative to gross volumetric evaluation of tumor response to therapy [12,13]. Many analytical techniques have been proposed for evaluating rCBV as an early response metric to treatment. The conventional approach for analyzing MRI parameters is to determine the percentage change in a summary statistic over the tumor VOI, which may be delineated using qualitative imaging such as T1-Gd and FLAIR images. These summary statistics may include the histogram mean, median, or even percentile of the parameter [14,15]. We have proposed a physiologically based approach where relative tumor volumes are determined from the segmentation of the tumor histogram based on known physiological values. The percentage changes in these relative volumes are determined from serially imaging examinations prior and following treatment initiation [12]. Finally, we have developed a new technique, called parametric response mapping (PRM), that monitors on a voxel-by-voxel basis regional changes in tumor perfusion for early assessment of therapeutic response in patients with glioma [16]. The PRM approach, when applied to rCBV (PRM_{rCBV}) within the enhancing tumor as contoured on T1-Gd images, has been shown to be highly predictive of survival as early as 1 week post-treatment initiation as well as differentiating pseudoprogression from true progression [12,16,17].

There exists a wide variety of techniques for analyzing rCBV data. The extensive research devoted to investigating rCBV as a surrogate imaging biomarker of glioma response to therapy highlights the need for consensus on the optimal method for analyzing this imaging technique. In this study, we investigate the impact of the analytic method when applied to rCBV data for assessing therapeutic induced response in patients with glioma. In addition, we evaluated for each metric the effect of both 1) the VOI used, Gd-VOI *versus* FLAIR-VOI, and 2) the time of MRI examination post-treatment initiation on the metrics predictive value of 1-year and overall survival in a cohort of patients with glioma.

Materials and Methods

Patients

Patients with pathologically proven grade III/IV gliomas (n = 8/36, respectively) were enrolled on a protocol of intratreatment MRI. Informed consent was obtained, and images and medical record use were approved by the Institutional Review Board. Forty-four patients were evaluated pre-therapy and 1 and 3 weeks after initiation of chemoradiation. This cohort, or a part of this cohort of patients, has been used previously in published work investigating the prognostic value of PRM applied to the individual parameters of apparent diffusion coefficient [18] and rCBV [16] and a composite model of PRM applied to these two parameters [19].

Radiotherapy was delivered over 6 weeks using standard techniques with a 2.0- to 2.5-cm margin on either the enhancing region on Gd-enhanced scans or the abnormal signal on T2-weighted scans to 46 to 50 Gy with the central gross tumor treated to a final median dose of 70 Gy.

MRI Scans

MRI scans were performed 1 week before and 1 and 3 weeks after initiation of therapy. All images were acquired on either a 1.5-T MRI system (General Electric Medical Systems, Milwaukee, WI; n = 30 patients) or a 3-T Philips Achieva system (Philips Medical Systems, Best, The Netherlands; n = 14 patients). The MRI protocol included FLAIR, DSC T2*-weighted imaging, and contrast-enhanced T1-weighted imaging.

Following the FLAIR acquisition, Gd diethylenetriamine pentaacetic acid was injected intravenously with a dose of 0.05 to 0.1 ml/kg to decrease the blood-brain barrier leakage impact on the rCBV measurement as recommended by Paulson and Schmainda [20]. Subsequently, a T1-Gd image was acquired. For DSC imaging, 14 to 20 slices of dynamic T2*-weighted images were acquired by a gradient-echo echo-planar imaging pulse sequence [repetition time (TR) = 1.5 to 2 seconds, echo time (TE) = 50 to 60 milliseconds, field of view = 220 × 220 mm^2, matrix = 128 × 128, flip angle = 60°, sensitivity encoding (SENSE) factor = 3 in phase-encode anterior-posterior direction and 4- to 6-mm thickness and 0-mm gap]. DSC-MRIs were acquired before and following a second dose of Gd diethylenetriamine pentaacetic acid, which was injected intravenously with a dose of 0.05 to 0.1 ml/kg as a bolus using a power injector at a rate of 2 ml/s, followed immediately by 15 ml of saline flush at the same rate.

CBV maps were generated from DSC T2*-weighted images as described previously [12]. To assess differences in tumor blood volume during radiotherapy and between patients, CBV maps were normalized to values within white matter regions contralateral to the tumor to generate the rCBV. For normalization, we used those white matter VOIs that were contralateral to the tumor, had received <30 Gy

accumulated dose, and were as large as possible while still avoiding regions with susceptibility artifacts and partial volume averaging.

Image Registration

All image data were registered to pre-treatment T1-Gd images using mutual information as an objective function and Nelder-Mead simplex as an optimizer [21]. Automatic registration of different and similar weighted serial MRI scans for the same patient was performed assuming a rigid body–geometry relationship. Following registration, brain tumor VOIs were manually contoured by a neuroradiologist over regions of the tumor that are hyperintense on FLAIR (FLAIR-VOI) and on T1-Gd images (Gd-VOI).

Image Analysis

Three post-processing approaches were assessed for monitoring therapeutic response using VOIs contoured on FLAIR and T1-Gd images. A statistical summary approach was performed by calculating the percentage change of the rCBV mean and median. Additionally, we evaluated the percentage change of the percentiles of the histogram, which also include, in increments of 10% [22], 25th, 75th, and 95th percentiles [23] (Figure 1*A*). We then evaluated a physiologically based approach. In brief, tumor rCBV histograms pre-treatment and mid-treatment were separated into three segments using discrete thresholds previously defined as >4 for the high rCBV region (approximately 2 SD greater than the mean in gray matter), 1.7 to 4 in the intermediate rCBV, and <1.7 but >0.2 (2 SD less than the mean of white matter) in the low rCBV region [12] (Figure 1*B*). Then, the percentage changes over time of the volume fraction of these three regions were calculated and named as follows: high rCBV, medium rCBV, and low rCBV, respectively. The final approach analyzed is the PRM *voxel-based approach* [16]. Briefly, PRM was performed on spatially registered serial rCBV maps by calculating the difference in the rCBV values of each voxel within the tumor. Voxels were designated in the following three categories: increased rCBV (PRM_{rCBV+}, red voxels), decreased rCBV (PRM_{rCBV-}, blue voxels), and no change (PRM_{rCBV0}, green voxels; Figure 1*C*). The threshold that designates a significant change in rCBV within a voxel beyond the effect of imaging noise was defined as ±1.2 as previously described [16]. In brief, thresholds were determined empirically from seven randomly selected subjects. For each subject, healthy contralateral brain tissue was contoured to generate registered rCBV values pre-treatment and mid-treatment. The 95% confidence intervals were determined by linear least-squares regression analysis and averaged over all seven subjects.

Statistical Analysis

All parameters were analyzed for each mid-treatment examination and VOI. A paired *t* test was used to 1) compare tumor volumes contoured on FLAIR and T1-Gd and 2) to compare tumor volumes as defined separately by FLAIR-VOI and Gd-VOI over time (week 0 *vs* week 1, week 0 *vs* week 3, and week 1 *vs* week 3). We performed receiver operating characteristic (ROC) curve analysis for correlation of the imaging parameters with subject survival 1 year from diagnosis. The area under the curve (AUC) was obtained to distinguish which continuous variables were predictive measures of outcome. For parameters that were found to be statistically significant by ROC analysis, optimal cutoffs were determined from ROC curves based on optimal values of sensitivity and specificity. The patient population was then stratified on the basis of the optimal cutoffs for each parameter. Overall survival was assessed for each parameter using Kaplan-Meier survival curves and the log-rank test or Cox regression analysis for multivariate analyses. All statistical computations were performed with a statistical software package (SPSS Software Products, Chicago, IL), and results were declared statistically significant at the two-sided 5% comparison-wise significance level ($P < .05$).

Results

Patient Population

A total of 44 subjects with high-grade glioma were accrued for this prospective study. Kaplan-Meier analysis revealed that the overall

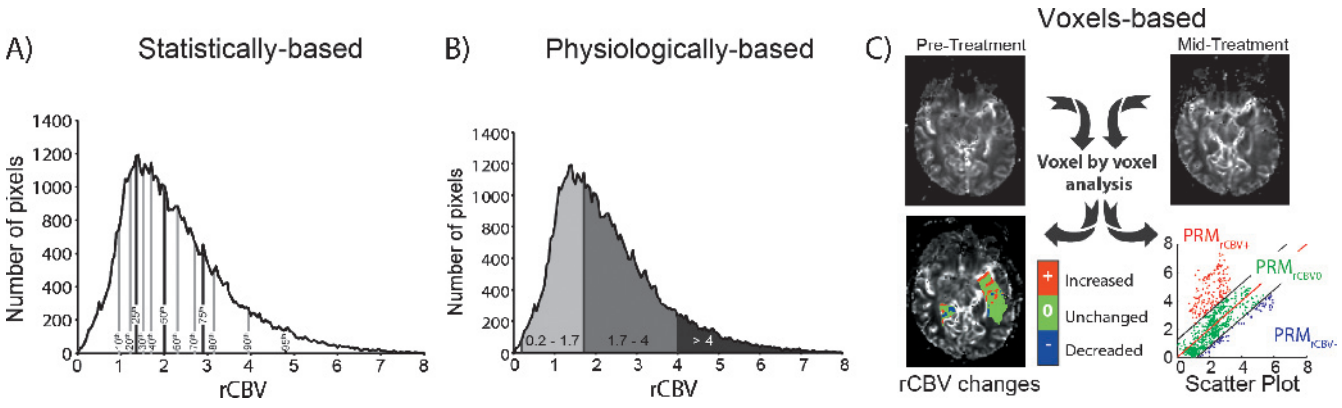

Figure 1. Schematic of histogram-based approach methods. (A) Statistical histogram-based segmentation consists of measuring the percentiles in increments of 10% plus 25th, 75th, and 95th percentiles. (B) Physiological histogram-based segmentation consists of measuring the tumor volume fraction with low rCBV (2 SD less than the mean of white matter), medium rCBV, or high rCBV (approximately 2 SD greater than the mean in gray matter) values. (C) Serial rCBV maps undergo digital image post-processing and analysis that involves registration of images before and during treatment. Once spatially aligned, individual voxels within the tumor are presented using a three-color overlay and are classified as unchanged (green), increased (red), or decreased (blue) rCBV following treatment initiation. These data can also be presented in a scatterplot and quantified over the entire tumor volume by summing all voxels within a classification and normalizing by the total tumor volume to generate relative volumes for each class.

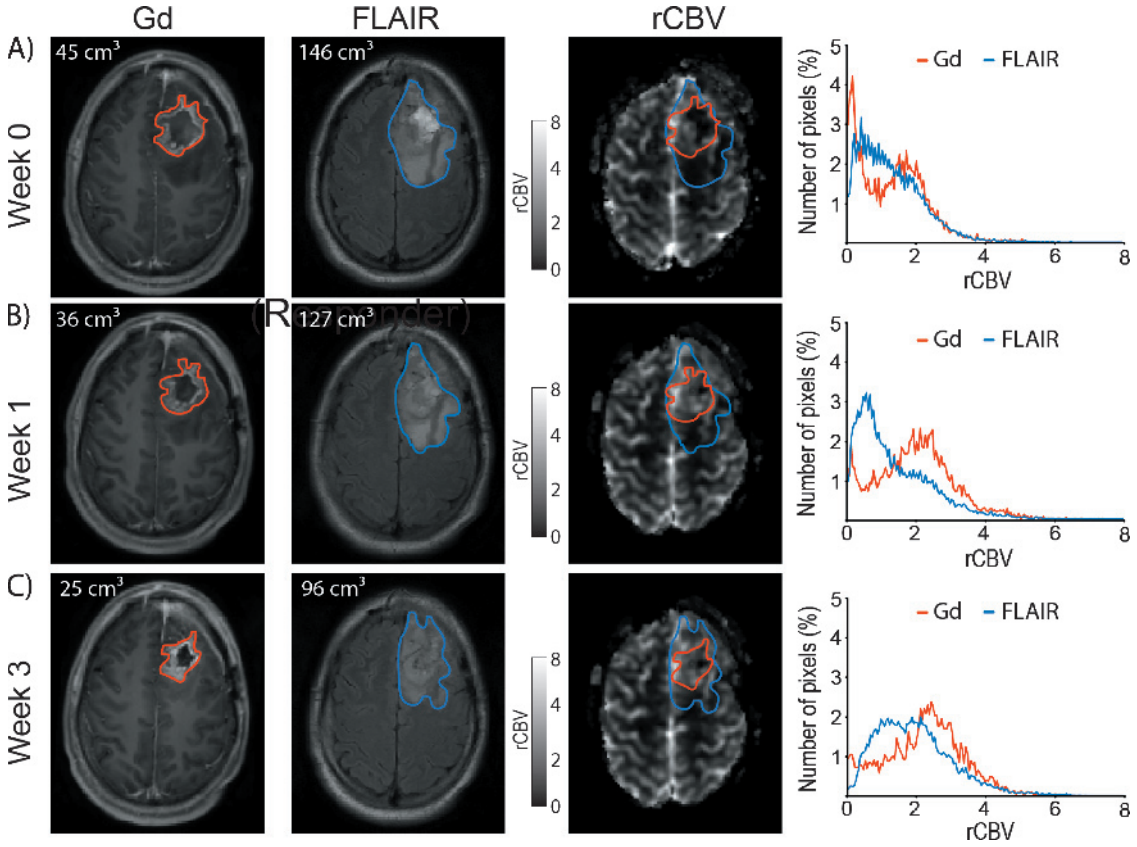

Figure 2. Representative T1-weighted post-Gd (left), FLAIR (middle), and rCBV maps (right) of a patient with glioblastoma at −1 (A), 1 (B), and 3 weeks (C) post-treatment initiation. Red and blue contours depict post-Gd T1-weighted and FLAIR imaging tumor volumes, respectively. The tumor histogram for rCBV is depicted using either Gd-VOI (red curves) or FLAIR-VOI (blue curves) obtained −1 (A), 1 (B), or 3 weeks (C) after treatment initiation.

median survival for this patient population was 13.1 months, with 52.3% of the population realizing 1-year survival.

Delineation and Characteristics of Tumor Volumes by MRI

Shrinkage or growth of the tumor during the time between scans may have occurred; however, for this patient population, no statistical changes in tumor volume were observed between week 0 and weeks 1 and 3 for Gd-VOI ($P = .89$ and $P = .38$, respectively) and between week 0 and week 3 for FLAIR-VOI ($P = .12$). Nevertheless, we observed a statically increase of the tumor size using the FLAIR-VOI between week 0 and week 1 (96 ± 71 *versus* 104 ± 84 cm^3, $P = .03$). Irrespective of the time of examination, mean tumor volume was statistically larger using the FLAIR-VOI compared to the Gd-VOI (FLAIR-VOI: 96 ± 71, 104 ± 84, and 105 ± 56 cm^3 *versus* Gd-VOI: 37 ± 29, 37 ± 31, and 35 ± 27 cm^3; before and 1 and 3 weeks after treatment onset, respectively; $P < .001$). In addition, we observed that tumor histograms were highly dependent on the VOI (Figure 2, *right column*; red *versus* blue curve).

Correlation of Image Analysis with Treatment Outcome

One-year survival was individually assessed for each metric, at each time point and VOI, using an ROC curve analysis (Table 1). As previously observed, PRM_{rCBV-} at 1 and 3 weeks mid-treatment using the Gd-VOI was predictive of survival at 1 year (Table 1) [16]. A new finding was that PRM_{rCBV-} based on the larger FLAIR-VOI was also predictive at weeks 1 and 3 (Table 1). In contrast, all statistically and physiologically based parameters failed to predict 1-year survival, and no further analysis was performed on these metrics (Table 1). Among all the failed metrics, only the low rCBV value using the FLAIR-VOI at week 3 mid-treatment was at the limit of significance ($P = .05$; Table 1).

Figures 3 and 4 provide representative PRM maps and corresponding scatterplots from therapeutically responding and nonresponding patients as determined by 1-year survival. PRM analyses for these two patients are presented for each time point during treatment and VOIs used in this study. For a representative responder patient, the relative volume of tumor with a significant drop in rCBV over time (PRM_{rCBV-}) was observed to be low for all time point VOIs used with a range of 1.3% to 1.8% (Figure 3, *A–D*, blue dots). In contrast, for a representative nonresponding patient, considerably more tumor volume was classified as PRM_{rCBV-} regardless of VOI and time point range was 14.4% to 26% (Figure 5, blue dots). This increase of PRM_{rCBV-} values corresponds to a decrease of rCBV within these voxels (blue voxels in Figures 3 and 4) during therapy.

Across the four conditions of two intervals (1 and 3 weeks) and VOIs (Gd and FLAIR), the optimal cutoffs for PRM_{rCBV-} to predict patient overall survival ranged from 4.6% to 6.8% that deviated by only 2.2% from the 6.8% previously reported [16] (Table 2). Subsequently, we used 5.9% (mean across the four optimal cutoffs) as the cutoff to stratify all patients within the population. The Kaplan-Meier survival curves and results from the log-rank tests are presented

Table 1. ROC Analysis Results at 1 or 3 Weeks Post-treatment Initiation Using Gd-VOI or FLAIR-VOI.

			Statistical			Physiological			PRM	
			Tumor Volume	rCBV Mean	rCBV Median	10th	20th	25th	30th	40th	50th	60th	70th	75th	80th	90th	95th	Low rCBV	Medium rCBV	High rCBV	PRM_{rCBV+}	PRM_{rCBV-}
Week 1	Gd	AUC	0.640	0.408	0.424	0.565	0.540	0.538	0.520	0.464	0.424	0.418	0.410	0.422	0.408	0.383	0.381	0.542	0.472	0.451	0.513	0.743
		P value	.113	.296	.391	.459	.647	.664	.823	.681	.391	.353	.307	.378	.296	.184	.177	.630	.751	.581	.879	.006
	FLAIR	AUC	0.615	0.607	0.569	0.551	0.576	0.588	0.602	0.598	0.569	0.582	0.592	0.605	0.625	0.615	0.625	0.638	0.573	0.588	0.518	0.727
		P value	.192	.226	.431	.565	.391	.318	.245	.264	.431	.353	.296	.404	.155	.192	.155	.118	.404	.118	.698	.010
Week 3	Gd	AUC	0.640	0.538	0.536	0.567	0.526	0.524	0.509	0.520	0.636	0.555	0.563	0.571	0.563	0.547	0.551	0.644	0.509	0.557	0.586	0.733
		P value	.113	.664	.681	.445	.769	.787	.916	.623	.681	.534	.474	.418	.474	.597	.565	.102	.916	.518	.329	.008
	FLAIR	AUC	0.524	0.588	0.571	0.576	0.569	0.576	0.582	0.598	0.571	0.580	0.573	0.582	0.584	0.569	0.555	0.673	0.547	0.513	0.534	0.749
		P value	.787	.318	.418	.391	.431	.391	.353	.285	.418	.366	.404	.353	.341	.431	.534	.050	.597	.879	.698	.005

AUC and *P* values were generated from the ROC analysis of every metric described in Materials and Methods section ($n = 20$). Metrics were grouped by methods: statistically, physiologically, and PRM voxel-based approaches. Only PRM_{rCBV-} metrics, using either the Gd-VOI or the FLAIR-VOI and every time mid-treatment, show a statistically significant ROC analysis.

for PRM_{rCBV-} analysis at weeks 1 and 3 for the T1-Gd and FLAIR-VOIs (Figure 5). Each of the four PRM_{rCBV-} graphs shows similar predictive value for the imaging biomarker as each approach was able to predict significantly different patient outcomes irrespective of the time the post-treatment rCBV map was acquired or the VOI used. Patients identified as responders by PRM irrespective of the examination time lived significantly longer compared to those identified as nonresponders (Figure 5). Although the parameter low rCBV, as defined by the physiologically based approach, using the FLAIR-VOI at week 3 mid-treatment did not fall within our criteria, nevertheless additional analysis was performed to assess predictive value for overall survival. Using a Kaplan-Meier analysis and log-rank test, this parameter was weakly predictive of overall survival ($P = .024$; data not show).

Bivariate Cox regression analyses were performed to compare low rCBV against PRM_{rCBV-} using the same VOI at the same examination time (i.e., FLAIR-VOI at 3 weeks). We observed that only the dichotomized variable of PRM_{rCBV-}, obtained using the 5.9% cutoff, was required to fit the statistical model to the survival data ($P = .002$). Low rCBV, dichotomized using the optimal cutoff of –2.2%, contributed to the Cox regression model ($P = .2$). In addition, we performed a multivariate Cox regression analysis to assess an optimal examination time and VOI for PRM analysis. Comparing the four different PRM_{rCBV-} graphs, dichotomized using the mean cutoff of 5.9% where all parameters were entered into the statistical model, did not result in a single significant parameter ($P > .2$).

Discussion

High-grade gliomas are markedly heterogeneous in their morphologic and genetic nature [24,25]. As such, they demonstrated a spatially heterogeneous response to cytotoxic and radiation therapies with tumor regions developing elevated levels of edema, necrosis, and even angiogenesis, adding difficulty in ascertaining treatment efficacy [26]. Advanced quantitative MRI techniques, such as DSC-MRI, have shown promise as a robust imaging technique for grading and response monitoring of tumors by focusing principally on a specific physiological feature of the tumor, in this case tumor blood volume [15,27]. Although physiological changes within the tumor following therapy can be visualized by quantitative MRI, the use of these techniques as a surrogate biomarker of patient survival continues to be hampered due to uncertainties in knowing how to optimally analyze the data to provide for the most predictive metric.

The traditional method of analyzing quantitative images is to calculate a scalar quantity, e.g., mean or median, that represents the physiological state of the entire tumor volume at a given time point. A positive or negative response of the tumor following a therapeutic intervention can be inferred from the percentage change in the quantitative scalar value, thus providing a biomarker that can be tested as a surrogate of patient survival and translated as a clinical end point [13,15,28–30]. Although these techniques can be applied quickly and easily by simply contouring the tumor volume, the metrics provided in our study failed to yield an accurate biomarker of response that can predict survival. One fundamental reason for this is that histogram-based approaches, whether statistical or physiological in nature, rely on tumor values where the sensitivity of the metric may attenuate consequent of the underlying heterogeneous response of the tumor mass. In this regard, we found that histogram-based techniques for image analysis showed negligible changes in rCBV when an increase in metric value in one tumor region was offset

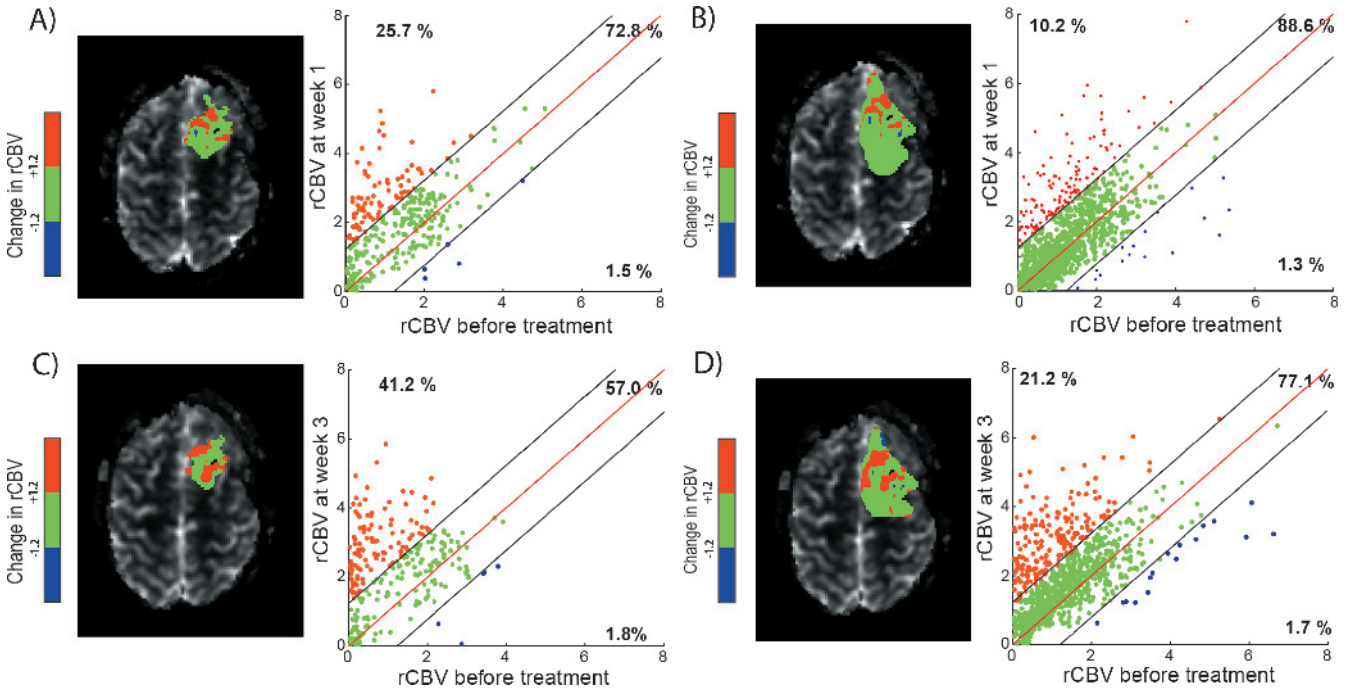

Figure 3. PRM_{rCBV} of a patient responsive to therapy with an overall survival of 22 months. Representative slice of PRM_{rCBV} color-coded VOI (A, C: Gd-VOI and B, D: FLAIR-VOI) superimposed onto an rCBV map (left) and the corresponding quantitative scatterplot analysis (right) showing the distribution or rCBV at baseline compared with mid-time treatment (A, B: week 1 and C, D: week 3). The values of PRM_{rCBV+}, PRM_{rCBV0}, and PRM_{rCBV-} of this patient (corresponding to the relative tumor volume of red, green, and blue voxel pairs plotted as dots, respectively) are presented in each scatterplot.

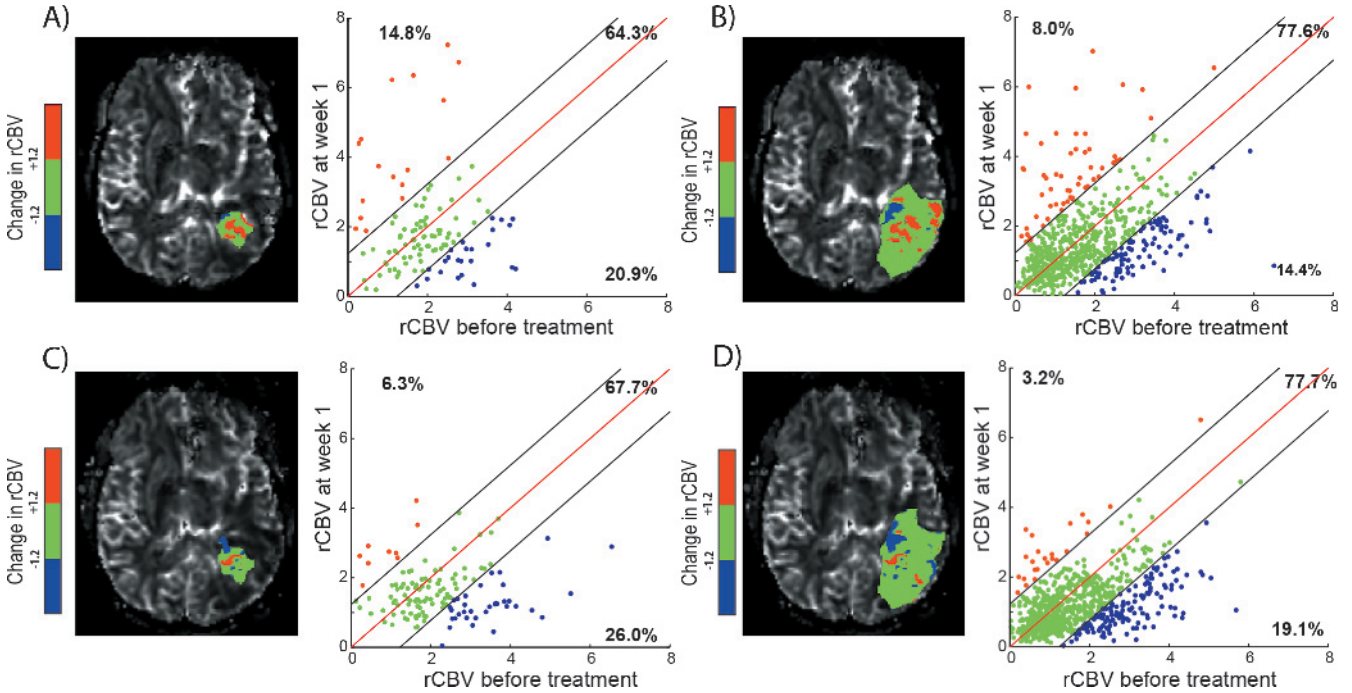

Figure 4. PRM_{rCBV} of a patient nonresponsive to therapy with an overall survival of 2.9 months. Representative slice of PRM_{rCBV} color-coded VOI (A, C: Gd-VOI and B, D: FLAIR-VOI) superimposed onto an rCBV map (left) and the corresponding quantitative scatterplot analysis (right) showing the distribution or rCBV at baseline compared with mid-time treatment (A, B: week 1 and C, D: week 3). For each scatterplot, the values of PRM_{rCBV+}, PRM_{rCBV0}, and PRM_{rCBV-} of this patient (corresponding to the relative tumor volume of red, green, and blue voxel pairs plotted as dots, respectively) are presented.

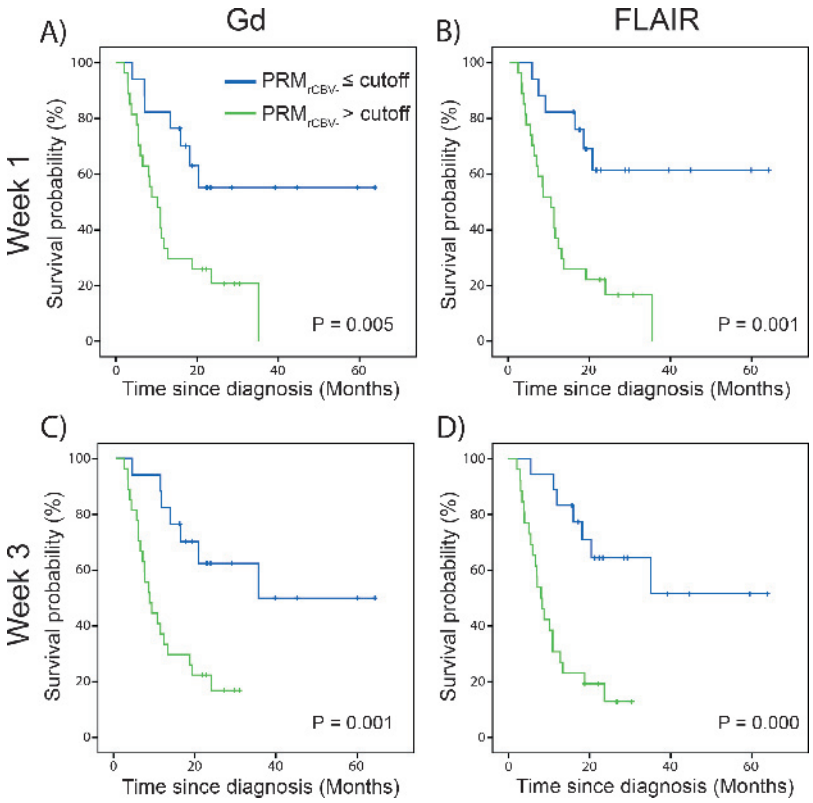

Figure 5. Predictive value of imaging biomarkers. Kaplan-Meier survival plots for overall survival, presented as stratified by PRM_{rCBV-} at (A, B) week 1 or (C, D) week 3 after treatment initiation and using either (A, C) Gd-VOI or (B, D) FLAIR-VOI. Blue line indicates PRM_{rCBV-} lower than or equal to the cutoff and green line indicates PRM_{rCBV-} more than the cutoff. The cutoff of 5.9% was defined as the mean of the optimal cutoff calculated for each PRM_{rCBV-} at a specific time interval post-therapy and VOI (Table 2).

by a decrease in another spatially distinct region. Assessing therapeutic response in patients with glioma using apparent diffusion coefficient (ADC) maps, Moffat et al. observed that tumor reaction to cytotoxic treatment was spatially dependent. This led to the development of the first voxel-based approach called the functional diffusion map [18]. This analysis was further applied to rCBV maps and has been shown to predict tumor response to standard therapy as well as distinguish progression from a pseudoprogression in high-grade gliomas [16,17]. In the present study, we have found that only the voxel-based approach, PRM, was sensitive enough to predict treatment response and that this sensitivity showed no dependence on time of mid-treatment acquisitions as well as tumor delineation. In general, patients who have a larger fraction of their tumor with decreased rCBV values do worse than patients who do not. One hypothesis for this finding may be that a rapid drop in rCBV leads to a volume fraction more likely to be hypoxic or alternatively to a reduction in the concentration of chemotherapeutic agent delivered to the tumor site and thus are more resistant to chemoradiotherapy. Nevertheless, evaluation of a variety of possible analytical techniques for assessing therapeutic response using a well-defined cohort of high-grade glioma (HGG) patients has provided unique insights into optimizing image analysis approaches for assessment of tumor response.

In this present study, we realized the importance of noncontrast-enhancing regions as defined by FLAIR as a complimentary metric to T1-Gd images for tumor response to therapy as highlighted by the RANO Working Group as well as the introduction of different analytical techniques for evaluating rCBV data. We demonstrated in a single site prospective clinical study that the PRM technique was able to provide a metric capable of early prediction of patient survival, whereas other analytical approaches showed no predictive potential. Although using the same cohort of patients, these new findings are distinctly different from results reported in our previous studies. First, among the different analytic methods tested at various mid-treatment time points and VOIs, only the PRM_{rCBV-} significantly correlated to patient survival. Previous analyses compared the predictive value of PRM_{rCBV-} only against the percentage change

Table 2. Survival Analysis.

Metric	Time Point (Weeks)	VOI (Mean Tumor Volume, cm^3)	AUC	ROC *P* Value	Cutoff	Log-Rank Test
PRM_{rCBV-}	1	Gd (37 ± 31)	0.754	.006	6.8	0.005
PRM_{rCBV-}	1	FLAIR (104 ± 84)	0.727	.01	4.6 (−32%)	<0.0001
PRM_{rCBV-}	3	Gd (35 ± 27)	0.733	.008	6.8 (0%)	<0.0001
PRM_{rCBV-}	3	FLAIR (105 ± 86)	0.749	.005	5.3 (−22%)	<0.0001

Note: Only metrics that could statistically predict 1-year survival, based on ROC curves, are presented and further analyzed.

in the mean rCBV. Second, this voxel-based approach was found to be very robust for patient treatment response stratification with negligible sensitivity in the optimal cutoff to the choice of VOI (volumes delineated by Gd or FLAIR) or the time the rCBV map was acquired during treatment (5.9 ± 1.1%; mean ± SD across optimal cutoffs for PRM_{rCBV-}). No such analysis was performed in our previous work. PRM analysis applied to rCBV was shown to be a flexible (VOI and time after start of treatment) and robust (a single cutoff is applicable) early imaging response biomarker for patients with brain tumors. Changes of tumor size over time are an important issue of the PRM technique and it needs to be carefully checked. In our study, no significant changes in tumor sizes were observed; the exception was the change in tumor volume as defined by FLAIR-VOI between weeks 0 and 1. We employed a rigid body registration algorithm for our PRM analysis of rCBV data. Although nonlinear deformation in the tumor may have occurred over the interval examinations, these changes were small relative to local changes in rCBV values. The rationale is that excessive deformation would cause erroneous PRM values eliminating any predictive potential and ultimately resulting in only noise from the PRM analysis. In fact, excessive imaging noise and artifacts would also result in errors in the PRM values. Contrary to all of this, PRM was the only metric predictive of overall survival. By applying these techniques to a single cohort, imaging noise, artifacts, and changes in tumor volume are essentially controlled. A multivariate Cox regression analysis was performed to evaluate the impact of the percentage change in tumor volume on the prediction of the PRM_{rCBV-} metric using the FLAIR-VOI at week 1. PRM_{rCBV-} was the only significant parameter for the regression model to predict overall patient survival ($P = .001$ and $P = .9$ for PRM_{rCBV-} and the percentage change in tumor volume, respectively). Moreover, in this same period, the percentage change of the tumor size was +6.5 ± 3.8% (mean ± SEM) and is on the same order as the interobserver variability for manual tracing of brain tumor (up to 15%) [31].

We have demonstrated that despite perfusion MRI showing promise as a surrogate biomarker of therapeutic response in patients with glioma, the choice of analytical method greatly impacts the sensitivity of the imaging biomarker. The PRM approach to analyzing imaging data improves the accuracy of perfusion MRI as a biomarker of overall survival but is also insensitive to tumor VOIs and mid-treatment time of acquisition. This study illustrates the importance of the analytical method for assessing early prediction of treatment response using MRI perfusion data. The application of PRM to blood perfusion maps shows promise as an early and robust surrogate imaging biomarker of treatment response in patients diagnosed with high-grade glioma.

References

[1] Porter KR, McCarthy BJ, Freels S, Kim Y, and Davis FG (2010). Prevalence estimates for primary brain tumors in the United States by age, gender, behavior, and histology. *Neuro Oncol* **12**, 520–527.

[2] Macdonald DR, Cascino TL, Schold SC Jr, and Cairncross JG (1990). Response criteria for phase II studies of supratentorial malignant glioma. *J Clin Oncol* **8**, 1277–1280.

[3] Wen PY, Macdonald DR, Reardon DA, Cloughesy TF, Sorensen AG, Galanis E, Degroot J, Wick W, Gilbert MR, Lassman AB, et al. (2010). Updated response assessment criteria for high-grade gliomas: response assessment in Neuro-Oncology Working Group. *J Clin Oncol* **28**, 1963–1972.

[4] Sorensen AG, Batchelor TT, Wen PY, Zhang WT, and Jain RK (2008). Response criteria for glioma. *Nat Clin Pract Oncol* **5**, 634–644.

[5] Henson JW, Ulmer S, and Harris GJ (2008). Brain tumor imaging in clinical trials. *AJNR Am J Neuroradiol* **29**, 419–424.

[6] Vos MJ, Uitdehaag BM, Barkhof F, Heimans JJ, Baayen HC, Boogerd W, Castelijns JA, Elkhuizen PH, and Postma TJ (2003). Interobserver variability in the radiological assessment of response to chemotherapy in glioma. *Neurology* **60**, 826–830.

[7] Stupp R, Mason WP, van den Bent MJ, Weller M, Fisher B, Taphoorn MJ, Belanger K, Brandes AA, Marosi C, Bogdahn U, et al. (2005). Radiotherapy plus concomitant and adjuvant temozolomide for glioblastoma. *N Engl J Med* **352**, 987–996.

[8] Bian W, Khayal IS, Lupo JM, McGue C, Vandenberg S, Lamborn KR, Chang SM, Cha S, and Nelson SJ (2009). Multiparametric characterization of grade 2 glioma subtypes using magnetic resonance spectroscopic, perfusion, and diffusion imaging. *Transl Oncol* **2**, 271–280.

[9] Schmainda KM, Rand SD, Joseph AM, Lund R, Ward BD, Pathak AP, Ulmer JL, Badruddoja MA, and Krouwer HGJ (2004). Characterization of a first-pass gradient-echo spin-echo method to predict brain tumor grade and angiogenesis. *AJNR Am J Neuroradiol* **25**, 1524–1532.

[10] Tunariu N, Kaye SB, and Desouza NM (2012). Functional imaging: what evidence is there for its utility in clinical trials of targeted therapies? *Br J Cancer* **106**, 619–628.

[11] Walker C, Baborie A, Crooks D, Wilkins S, and Jenkinson MD (2011). Biology, genetics and imaging of glial cell tumours. *Br J Radiol* **84**, S90–S106.

[12] Cao Y, Tsien CI, Nagesh V, Junck L, Ten Haken R, Ross BD, Chenevert TL, and Lawrence TS (2006). Survival prediction in high-grade gliomas by MRI perfusion before and during early stage of RT [corrected]. *Int J Radiat Oncol Biol Phys* **64**, 876–885.

[13] Pope WB, Kim HJ, Huo J, Alger J, Brown MS, Gjertson D, Sai V, Young JR, Tekchandani L, Cloughesy T, et al. (2009). Recurrent glioblastoma multiforme: ADC histogram analysis predicts response to bevacizumab treatment. *Radiology* **252**, 182–189.

[14] Mangla R, Singh G, Ziegelitz D, Milano MT, Korones DN, Zhong J, and Ekholm SE (2010). Changes in relative cerebral blood volume 1 month after radiation-temozolomide therapy can help predict overall survival in patients with glioblastoma. *Radiology* **256**, 575–584.

[15] Sawlani RN, Raizer J, Horowitz SW, Shin W, Grimm SA, Chandler JP, Levy R, Getch C, and Carroll TJ (2010). Glioblastoma: a method for predicting response to antiangiogenic chemotherapy by using MR perfusion imaging—pilot study. *Radiology* **255**, 622–628.

[16] Galbán CJ, Chenevert TL, Meyer CR, Tsien C, Lawrence TS, Hamstra DA, Junck L, Sundgren PC, Johnson TD, Ross DJ, et al. (2009). The parametric response map is an imaging biomarker for early cancer treatment outcome. *Nat Med* **15**, 572–576.

[17] Tsien C, Galbán CJ, Chenevert TL, Johnson TD, Hamstra DA, Sundgren PC, Junck L, Meyer CR, Rehemtulla A, Lawrence T, et al. (2010). Parametric response map as an imaging biomarker to distinguish progression from pseudoprogression in high-grade glioma. *J Clin Oncol* **28**, 2293–2299.

[18] Moffat BA, Chenevert TL, Lawrence TS, Meyer CR, Johnson TD, Dong Q, Tsien C, Mukherji S, Quint DJ, Gebarski SS, et al. (2005). Functional diffusion map: a noninvasive MRI biomarker for early stratification of clinical brain tumor response. *Proc Natl Acad Sci USA* **102**, 5524–5529.

[19] Galban CJ, Chenevert TL, Meyer CR, Tsien C, Lawrence TS, Hamstra DA, Junck L, Sundgren PC, Johnson TD, Galban S, et al. (2011). Prospective analysis of parametric response map-derived MRI biomarkers: identification of early and distinct glioma response patterns not predicted by standard radiographic assessment. *Clin Cancer Res* **17**, 4751–4760.

[20] Paulson ES and Schmainda KM (2008). Comparison of dynamic susceptibility-weighted contrast-enhanced MR methods: recommendations for measuring relative cerebral blood volume in brain tumors. *Radiology* **249**, 601–613.

[21] Meyer CR, Boes JL, Kim B, Bland PH, Zasadny KR, Kison PV, Koral K, Frey KA, and Wahl RL (1997). Demonstration of accuracy and clinical versatility of mutual information for automatic multimodality image fusion using affine and thin-plate spline warped geometric deformations. *Med Image Anal* **1**, 195–206.

[22] Li KL, Wilmes LJ, Henry RG, Pallavicini MG, Park JW, Hu-Lowe DD, McShane TM, Shalinsky DR, Fu YJ, Brasch RC, et al. (2005). Heterogeneity in the angiogenic response of a BT474 human breast cancer to a novel vascular endothelial growth factor-receptor tyrosine kinase inhibitor: assessment by voxel analysis of dynamic contrast-enhanced MRI. *J Magn Reson Imaging* **22**, 511–519.

[23] Barajas RF, Rubenstein JL, Chang JS, Hwang J, and Cha S (2010). Diffusion-weighted MR imaging derived apparent diffusion coefficient is predictive of

clinical outcome in primary central nervous system lymphoma. *AJNR Am J Neuroradiol* **31**, 60–66.

[24] Tate MC and Aghi MK (2009). Biology of angiogenesis and invasion in glioma. *Neurotherapeutics* **6**, 447–457.

[25] Sadeghi N, D'Haene N, Decaestecker C, Levivier M, Metens T, Maris C, Wikler D, Baleriaux D, Salmon I, and Goldman S (2008). Apparent diffusion coefficient and cerebral blood volume in brain gliomas: relation to tumor cell density and tumor microvessel density based on stereotactic biopsies. *AJNR Am J Neuroradiol* **29**, 476–482.

[26] Ananthnarayan S, Bahng J, Roring J, Nghiemphu P, Lai A, Cloughesy T, and Pope WB (2008). Time course of imaging changes of GBM during extended bevacizumab treatment. *J Neurooncol* **88**, 339–347.

[27] Lemasson B, Serduc R, Maisin C, Bouchet A, Coquery N, Robert P, Le Duc G, Tropres I, Remy C, and Barbier EL (2010). Monitoring blood-brain barrier status in a rat model of glioma receiving therapy: dual injection of low-molecular-weight and macromolecular MR contrast media. *Radiology* **257**, 342–352.

[28] Provenzale JM, Mukundan S, and Barboriak DP (2006). Diffusion-weighted and perfusion MR imaging for brain tumor characterization and assessment of treatment response. *Radiology* **239**, 632–649.

[29] Young R, Babb J, Law M, Pollack E, and Johnson G (2007). Comparison of region-of-interest analysis with three different histogram analysis methods in the determination of perfusion metrics in patients with brain gliomas. *J Magn Reson Imaging* **26**, 1053–1063.

[30] Mayr NA, Yuh WTC, Jajoura D, Wang JZ, Lo SS, Montebello JF, Porter K, Zhang D, McMeekin DS, and Buatti JM (2010). Ultra-early predictive assay for treatment failure using functional magnetic resonance imaging and clinical prognostic parameters in cervical cancer. *Cancer* **116**, 903–912.

[31] Kaus MR, Warfield SK, Nabavi A, Black PM, Jolesz FA, and Kikinis R (2001). Automated segmentation of MR images of brain tumors. *Radiology* **218**, 586–591.